Journal of Orthopaedic Surgery and Research

RESEARCH

Open Access

Inhibition of id-1 reduces osteosarcoma growth and metastasis through mediation of snail

Rongbing Shu[1†], Zhuanyi Yu[1†], Jianmin Wu[1], Qiuxin Cheng[1], Zhihao Peng[1], Huaqiang Zhou[1] and Min Zhao[1*]

Abstract

Objective Osteosarcoma (OS) is a highly invasive bone tumor that frequently metastasizes to the lungs. This study aims to investigate the role of the Id-1 gene in OS invasion and metastasis, and its relationship with the Snail gene.

Methods This study included tissue samples from 12 non-metastatic osteosarcomas and 9 metastatic osteosarcoma patients to examine the expression of Id-1 and Snail using RT-qPCR and analyze their correlation. In cell-based experiments, four osteosarcoma cell lines (Saos-2, U2OS, MG-63, and 143B) and the human osteoblast cell line hFOB 1.19 were cultured. The expression of Id-1 and Snail was evaluated by RT-qPCR and Western blotting.Cells were randomly divided into the Control group, sh-NC group, and sh-Id-1 group using lentiviral infection. Transwell invasion and scratch assays were used to assess cell migration and invasion. WB was employed to detect the expression of Id-1, Snail, and epithelial-mesenchymal transition (EMT)-related proteins (E-cadherin, vimentin, and N-cadherin) in the OS cells of each group. In animal experiments, Tumor formation in each group was evaluated by injecting cells subcutaneously into mice. An osteosarcoma lung metastasis model was established by injecting infected cells into the tibia of mice. Tumor growth and lung metastasis were observed using HE staining. The expression of Id-1, Snail, and EMT-related proteins in osteosarcoma and lung tissues from each group of mice was assessed using Western blot and immunohistochemistry.

Results The expression of Id-1 and Snail was significantly higher in osteosarcoma tissues than in normal bone tissues, and the expression of Id-1 was positively correlated with that of Snail. In cell experiments, downregulation of Id-1 reduced Snail expression and significantly inhibited EMT, as well as the migration and invasion of OS cells ($P < 0.05$). In animal experiments, compared to the Control group, the sh-Id-1 group mice was no significant change in body weight, but the tumor volume was significantly reduced, and fewer lung metastatic nodules ($P < 0.05$). HE staining indicated decreased nuclear atypia, reduced invasion and destruction, fewer new blood vessels, and less calcification in the sh-Id-1 group tumors. Immunohistochemistry and WB results showed upregulation of E-cadherin and downregulation of vimentin, N-cadherin, Id-1, and Snail in the sh-Id-1 group ($P < 0.05$).

†Rongbing Shu and Zhuanyi Yu have contributed equally to this work and share first authorship.

*Correspondence:
Min Zhao
zhaominytrmyy@sina.com

Full list of author information is available at the end of the article

Conclusion Downregulation of Id-1 inhibits the EMT process by reducing Snail expression, effectively suppressing the growth, invasion, and lung metastasis of OS.

Keywords Id-1, Snail, Osteosarcoma, EMT, Metastasis

Introduction

Osteosarcoma (OS) is a highly malignant bone tumor and the most common type of bone cancer [1]. It poses significant threats to patients, severely affecting limb function and quality of life [2]. OS predominantly occurs in adolescents and is characterized by high invasiveness and a propensity for distant metastasis, particularly to the lungs [3]. Despite recent improvements in patient prognosis through combined chemotherapy and surgical treatments, the high recurrence and metastasis rates of OS still result in poor outcomes [4]. The five-year survival rate for patients with metastatic or recurrent disease remains below 30% [5]. Therefore, understanding the molecular mechanisms underlying OS metastasis is a crucial focus in OS research, with significant implications for preventing and treating OS invasion and metastasis, and for improving survival rates.

Research has confirmed that epithelial-mesenchymal transition (EMT) of cancer cells is a key initial step in their recurrence and metastasis [6, 7]. During this transition, cancer cells lose their epithelial characteristics and gain mesenchymal traits, which enhance their invasiveness and migratory capabilities [8]. However, the intricate signaling pathways involved in this process in OS remain unclear. Inhibitor of differentiation protein 1 (Id-1) is an important transcriptional regulator that influences cell proliferation, differentiation, and apoptosis [9–11]. Previous studies have shown that Id-1 is highly expressed in various tumors and is closely associated with tumor invasion and metastasis [12]. Research by Luo et al. Demonstrated that the Id-1 gene affects the expression of EMT markers in tongue squamous cell carcinoma (TSCC) cells [13]. Zinc finger transcription factor (Snail), a key transcription factor promoting the EMT process, facilitates cancer cell migration and invasion by downregulating E-cadherin and upregulating mesenchymal markers such as vimentin and N-cadherin [14, 15]. However, the specific roles and interactions of Id-1 and Snail in OS remain unclear.

This study aims to explore the role of Id-1 in OS invasion and metastasis and its relationship with the Snail gene. Through these investigations, we hope to elucidate the specific mechanisms of Id-1 in OS, providing new insights and theoretical bases for the prevention and targeted treatment of OS.

Methods

Reagents

Mammalian shRNA interference lentiviral vector (VB010000, VectorBuilder, Guangzhou, China); Fetal Bovine Serum (FBS, F0193, Merck, Darmstadt, Germany); Penicillin-Streptomycin (TMS-AB2, Merck, Darmstadt, Germany); Dulbecco's Modified Eagle Medium/Nutrient Mixture F-12 (DMEM/12F) (12634028, ThermoFisher, Waltham, MA, USA); Minimum Essential Medium (MEM, PM150410, Procell, Wuhan, China); McCoy's 5 A (Modified) medium (16600082, ThermoFisher, Waltham, MA, USA); Trypsin solution (T4299, Merck, Darmstadt, Germany); 4% Paraformaldehyde Fixative (P0099, Beyotime, Shanghai, China); Crystal Violet (32675, Merck, Darmstadt, Germany); Phosphate Buffer Saline (PBS, 10010001, ThermoFisher, Waltham, MA, USA); Pentasorbital Sodium (P3761, Merck, Darmstadt, Germany); Hematoxylin Eosin (HE) Staining Kit (C0105S, Beyotime, Shanghai, China); 10% Bovine Serum Albumin (BSA, V900933, Merck, Darmstadt, Germany); Diaminobenzidine (DAB, D5905, Merck, Shanghai, China); RIPA Lysis Buffer (P0013B, Beyotime, Shanghai, China); BCA Protein Quantification Kit (P0009, Beyotime, Shanghai, China); Polyacrylamide Gel (SDS-PAGE, NP0007, ThermoFisher, Waltham, MA, USA); Polyvinylidene Fluoride (PVDF) Membrane (FFP70, Beyotime, Shanghai, China); Tris Buffered Saline with Tween-20 (TBST) Solution (786–1742, G-biosciences, Shanghai, China); BeyoECL Star (P0018S, Beyotime, Shanghai, China); RNA Extraction Kit (RC112-01, Vazyme, Nanjing, China); PrimeScript™ RT reagent Kit (RR037Q, Takara, Kyoto, Japan); Hieff® qPCR SYBR Green Master Mix (11201ES03, yeasen, Shanghai, China).

Clinical experiment

This study included 21 surgical resection samples, comprising 12 non-metastatic OS tissue samples and 9 lung metastatic OS tissue samples, from patients treated at our hospital between February 2021 and August 2023. All patients provided informed consent, and the study was conducted under the supervision of the Ethics Committee of Yingtan People's Hospital (YT2024101). Quantitative reverse transcription PCR (RT-qPCR) was used to detect the mRNA expression levels of Id-1 and Snail in non-metastatic and lung metastatic OS samples, and the correlation between Id-1 and Snail expression in lung metastatic OS was analyzed.

Cell culture and treatment

Saos-2 (CL0271), MG-63 (CL0217), 143B (CL0441) OS cell lines, and human osteoblast cell line (hFOB 1.19, CL0140) were procured from fenghbio (Changsha, China). OS cell line U2OS (SNL-054) were procured from sunncell (Wuhan, China). The cells were cultured in an appropriate medium containing 10% fetal bovine serum and 1% penicillin-streptomycin. Saos-2 and U2OS cells were cultured in McCOY's 5 A medium. MG-63 and 143B cells were cultured in MEM medium. hFOB 1.19 cells were cultured in DMEM/F12 medium. The cells were incubated in a humidified environment at 37 °C with 5% CO_2.

Constructing cells with stable gene transfection

The shRNA targeting Id-1 (sh-Id-1) and the negative control for lentivirus infection (sh-NC) were purchased from Vectorbuilder (Guangzhou, China) (Vector Name: pLV[shRNA]-Neo-U6 > hID1[shRNA#1]). Human osteosarcoma cell line MG-63 was inoculated into culture dishes and lentiviral infection was performed when the cells reached 60% fusion. sh-Id-1 (1, 2, 3#) and sh-NC were transfected into MG-63 cells, and the target sequences are shown in Table 1. After 48 h of infection, stable infected cells were screened by adding neomycin, and the success of gene expression changes was confirmed by RT-qPCR analysis.

Cell scratch assay

Each group of MG-63 was seeded at 2 × 10^4 cells/well in 24-well plates and cultured to confluence. The medium was aspirated, and cells were scratched with a 10 μL pipette tip. Cells were washed with PBS and incubated in a humidified environment at 37 °C with 5% CO_2. Scratch images were taken at 0 and 24 h using a phase-contrast microscope with a built-in digital camera. The wound healing rate was calculated using ImageJ software to analyze the scratch area. The wound healing rate was determined by the formula:

$$\text{Wound healing rate} = \frac{Initial\ scratch\ area\ -\ Scratch\ area\ at\ 24\ hours}{Initial\ scratch\ area} \times 100$$

Transwell assay

Cell invasion was measured using the QCM™ Cell Invasion Assay Kit (ECM551, Merck, Shanghai, China) according to the manufacturer's instructions. Cells from each group were plated in the upper chamber of a membrane coated with polymerized collagen. The medium in the upper chamber contains low-serum concentration. Complete medium was placed in the lower chamber. After incubation at 37 °C for 24 h, cells that had invaded to the lower surface of the membrane were extracted and counted using a standard microplate reader (at 560 nm). Data are presented as the percentage of invasion relative to the control group.

Table 1 The target sequences of shRNAs

shRNA ID	Target sequence
sh-Id-1 1#	CTTCGGGCTTCCACCTCATTT
sh-Id-1 2#	TTCCACTCGTGTGTTTCTATT
sh-Id-1 3#	*CGTTTGGTGCTTCTCAGATTT*

Animal experiments

Thirty-six Specific Pathogen-Free (SPF) 6-week-old male BALB/c nude mice (17–21 g) were purchased from Hunan Slake Kingda Laboratory Animal Co., Ltd. (Production License No.: SCXK [Hunan] 2016-0002). Mice were acclimatized for seven days in a suitable environment (18–26 °C temperature, 40–70% relative humidity, 12-hour light/dark cycle, free access to food and water) before the experiment. This study strictly adhered to the 3R principle and was approved by the Animal Committee of Yingtan People's Hospital (Ethics No.YT202413).

Eighteen mice were randomized into three groups ($n = 6$): Control, sh-NC, and sh-Id-1. The tumorigenic ability of OS cells was analyzed by constructing a subcutaneous tumor model. The stable infected cell lines from each group were resuspended in PBS, and the cell concentration was adjusted to 1×10^7 cells/mL. The cell suspension (100 μL per mouse) was then subcutaneously injected into the mice. Mice were weighed once a week, and tumor volume was measured by calculating the long (L) and short (W) diameters. Tumor volume ($V = \frac{L \times W^2}{2}$). When the tumor volume in the Control group reached 1000 mm^3, at week four, All mice were euthanized by intraperitoneal injection of pentobarbital sodium (150 mg/kg)., and collecting tumor tissue.

Eighteen mice were randomized into three groups ($n = 6$): Control, sh-NC, and sh-Id-1. Construction of an OS lung metastasis model by injecting OS cells into mouse tibiae. Mice were anesthetized with sodium pentasorbital (30 mg/kg) via intramuscular injection. After the mice lost their pain response, a 1 cm longitudinal incision was made at the proximal end of the right tibia under a surgical microscope (8× magnification). The skin was incised to expose the proximal tibia, and a 1 mL syringe was used to penetrate the bone cavity. A mouse osteosarcoma lung metastasis model was constructed by injecting 5 μL of stably infected cells (2 × 10^6 cells/5 μL) from each group into the tibia of mice. The skin was closed with 5 – 0 surgical sutures. The entire procedure was performed in a sterile environment [16]. The mice were euthanized, and lung tissues were collected in the fifth week. Lung metastasis nodules on the surface were counted visually.

HE staining

Mouse tissues were fixed in 10% formalin for 24 h. The fixed tissue samples were then dehydrated and cleared through graded ethanol and xylene, followed by embedding in paraffin. The paraffin-embedded tissues were sectioned into 5 μm thick slices using a microtome. The paraffin sections were deparaffinized in xylene and rehydrated through graded ethanol to water, then stained with hematoxylin and eosin. After staining, the sections were dehydrated and cleared again using graded ethanol and xylene. Finally, it was observed under a light microscope after sealing the film by resin.

Immunohistochemistry

Paraffin sections of lung tissue from mice with lung metastasis were baked at 55 °C for 30 min in a constant temperature oven, followed by deparaffinization in xylene and a graded ethanol series. Endogenous peroxidase was eliminated by treatment with a 3% hydrogen peroxide solution. The sections were then sealed in 10% BSA for 1 h. Subsequently, the sections were incubated with specific primary antibodies against Id-1 (1:100, ab230679, abcam, Cambridge, England), Snail (1:100, A5243, ABclonal, Wuhan, China), E-cadherin (1:100, A3044, ABclonal, Wuhan, China), vimentin (1:1000, A19607, ABclonal, Wuhan, China), and N-cadherin (1:100, A3045, ABclonal, Wuhan, China) at 4 °C overnight, followed by incubation with HRP-conjugated secondary antibodies (1:10,000, 31460, ThermoFisher, Waltham, MA, USA) at room temperature for 30 min. DAB was used for chromogenic staining, followed by counterstaining with hematoxylin. Imaging was performed using a digital confocal microscope (STELLARIS 8, Leica, Wetzlar, Germany).

WB

Total protein was extracted from tissue and cells using RIPA lysis buffer. The protein concentration was determined using a BCA protein quantification kit. Subsequently, the protein samples were loaded onto an SDS-PAGE gel for electrophoretic separation. The separated proteins were transferred to a PVDF membrane, which was subsequently blocked with 5% non-fat milk. The membrane was incubated overnight at 4 °C with primary antibodies against Id-1 (1:500, A8432, ABclonal, Wuhan, China), Snail (1:1000, A5243, ABclonal, Wuhan, China), E-cadherin (1:1000, A24874, ABclonal, Wuhan, China), vimentin (1:20,000, A19607, ABclonal, Wuhan, China), N-cadherin (1:1000, A3045, ABclonal, Wuhan, China) and GAPDH (1:50000, A19056, ABclonal, Wuhan, China). This was followed by incubation with HRP-conjugated secondary antibodies at room temperature for 2 h. The membrane was washed with TBST solution for 5 min, and bands were detected using BeyoECL Star for 30 s. Band intensity was analyzed using ImageJ software (V1.8.0.112, NIH, Madison, WI, USA). GAPDH was used as an internal reference for quantitative analysis.

Table 2 Primer sequences

Gene	direction	Sequence (5′-3′)
Id-1	F	AAACGTGCTGCTCTACGACA
	R	GGAACGCATGCCGCCT
Snail	*F*	*CGAGTGGTTCTTCTGCGCTA*
	R	*GGGCTGCTGGAAGGTAAACT*
GAPDH	*F*	*AATGGGCAGCCGTTAGGAAA*
	R	*GCGCCCAATACGACCAAATC*

RT-qPCR

Total RNA was extracted from homogenized tissue or cells using an RNA extraction kit according to the manufacturer's instructions. Suitable RNA was then reverse-transcribed to obtain cDNA, which was subjected to PCR reactions according to the instructions provided. The relative expression levels of target genes were analyzed using the comparative threshold method ($2^{-\Delta\Delta Ct}$ method). The design of PCR primers is listed in Table 2. GAPDH was used as an internal reference for quantitative analysis.

Statistical analysis

Statistical analysis was performed using Prism 9 software and data are expressed as mean ± standard deviation. Correlation analysis was performed using Pearson's correlation analysis. Differences between groups were analyzed by t-test, and comparisons involving three or more groups were analyzed by one-way ANOVA and two-way ANOVA, followed by Tukey's post hoc test. *p*-values less than 0.05 were considered statistically significant.

Results

Id-1 is highly expressed in metastatic osteosarcoma

To investigate the expression of Id-1 in osteosarcoma, we assessed Id-1 levels in 12 cases of non-metastatic osteosarcoma tissues and 9 cases of metastatic osteosarcoma tissues. As shown in Fig. 1A, RT-qPCR results revealed that Id-1 expression was significantly higher in metastatic osteosarcoma tissues compared to Non-metastatic tissues ($P < 0.0001$). Subsequently, we further validated these findings in cell experiments, which demonstrated that both mRNA and protein levels of Id-1 were markedly elevated in osteosarcoma cells compared to normal osteoblasts (Fig. 1B, C) ($P < 0.05$).

Snail is highly expressed in OS and is significantly correlated with the expression of Id-1

Based on the higher expression of Id-1 in metastatic osteosarcoma, we hypothesized that Id-1 may be associated with osteosarcoma metastasis. Snail is a key transcription factor regulating cellular EMT, and studies

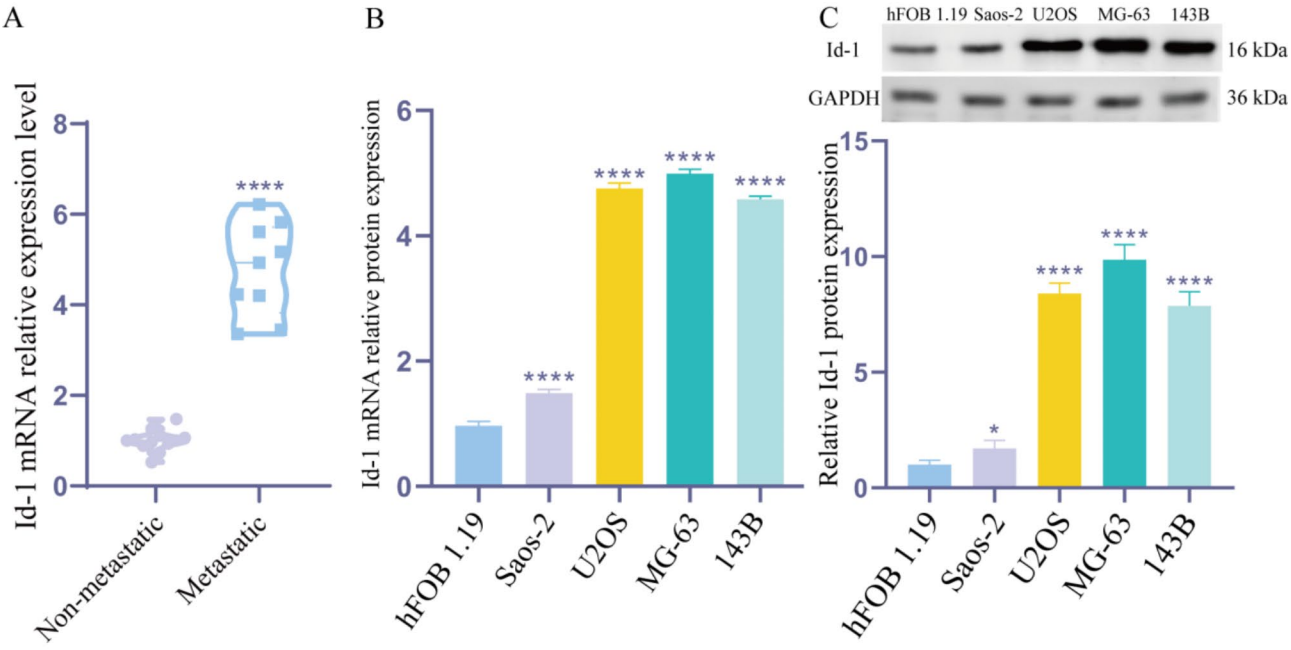

Fig. 1 Id-1 is highly expressed in metastatic osteosarcoma. (**A**) RT-qPCR detection of Id-1 mRNA expression, (Non-metastatic, $n=12$; Metastatic, $n=9$), data results were analyzed using t-test, ****$p<0.0001$ vs. non-metastatic; (**B**) RT-qPCR for Id-1 mRNA expression; (**C**) WB for Id-1 protein content. $n=3$, data results were analyzed using one-way ANOVA, *$p<0.05$ vs. hFOB1.19, ****$p<0.0001$ vs. hFOB1.19

have shown that Snail is closely associated with cancer migration and invasion [17]. Therefore, we hypothesize that Id-1 may affect the migration and invasion of osteosarcoma by influencing the expression of Snail. We analyzed the correlation between Id-1 and Snail in sarcoma using GEPIA (http://gepia.cancer-pku.cn/detail.php), and the results revealed a significant correlation between the two (Fig. 2A) ($P<0.05$, $r=0.42$). We further examined Snail expression in 12 non-metastatic and 9 metastatic osteosarcoma tissues, and the results showed that Snail mRNA expression was significantly higher in metastatic osteosarcoma tissues compared to non-metastatic ones (Fig. 2B) ($P<0.0001$). Subsequently, we validated the correlation between Id-1 and Snail in metastatic osteosarcoma, which also demonstrated a significant correlation (Fig. 2C) ($P<0.05$, $r=0.6824$). Additionally, we assessed Snail expression in osteosarcoma cell lines, revealing that Snail expression in osteosarcoma cells was significantly higher than in normal osteoblasts (Fig. 2D, E) ($P<0.05$), with the highest expression observed in the MG-63 cell line. Therefore, we selected the MG-63 cell line for subsequent experiments.

Silencing Id-1 reduces snail expression and inhibits EMT in OS cells

To investigate the effect of Id-1 on EMT, Id-1 was silenced in MG-63 cells by lentiviral transfection. RT-qPCR results showed that silencing Id-1 significantly decreased both Id-1 and Snail mRNA and protein expression in MG-63 cells, with sh-Id-1 2# exhibiting the highest interference efficiency (Fig. 3A) ($P<0.01$). Therefore, sh-Id-1 2# was selected for subsequent experiments. The results of RT-qPCR and WB showed that silencing of Id-1 significantly reduced the expression of Id-1 and Snail (Fig. 3A-B) ($P<0.01$). Next, we assessed cell proliferation using the MTT assay, and the results demonstrated that downregulation of Id-1 significantly inhibited the proliferation of tumor cells (Fig. 3C) ($P<0.0001$). In addition, down-regulation of Id-1 significantly promoted the expression of E-cadherin and suppressed the expression of vimentin and N-cadherin (Fig. 3D) ($P<0.01$). Next, We evaluated the effects of Id-1 silencing on migration and invasion of MG-63 cells by scratch assay and Transwell assay. The results showed that the migration and invasion of MG-63 cells were significantly decreased by Id-1 silencing (Fig. 3E-F) ($P<0.01$). These results suggest that silencing Id-1 significantly reduced Snail expression and inhibited the EMT process in OS cells.

Downregulation of Id-1 can improve the growth of subcutaneous tumors and lung metastasis in OS mice

The effect of Id-1 on lung metastasis and pathological characteristics was studied by injecting lentivirus-infected OS cells subcutaneously into mice. We first assessed the expression levels of Id-1 and Snail in subcutaneous tumor tissues using RT-qPCR and Western blot. The results showed that, compared to the sh-NC group, the expression levels of Id-1 and Snail were significantly decreased in the sh-Id-1 group (Fig. 4A-B). As shown in Fig. 4C, compared to the Control group, the sh-NC group

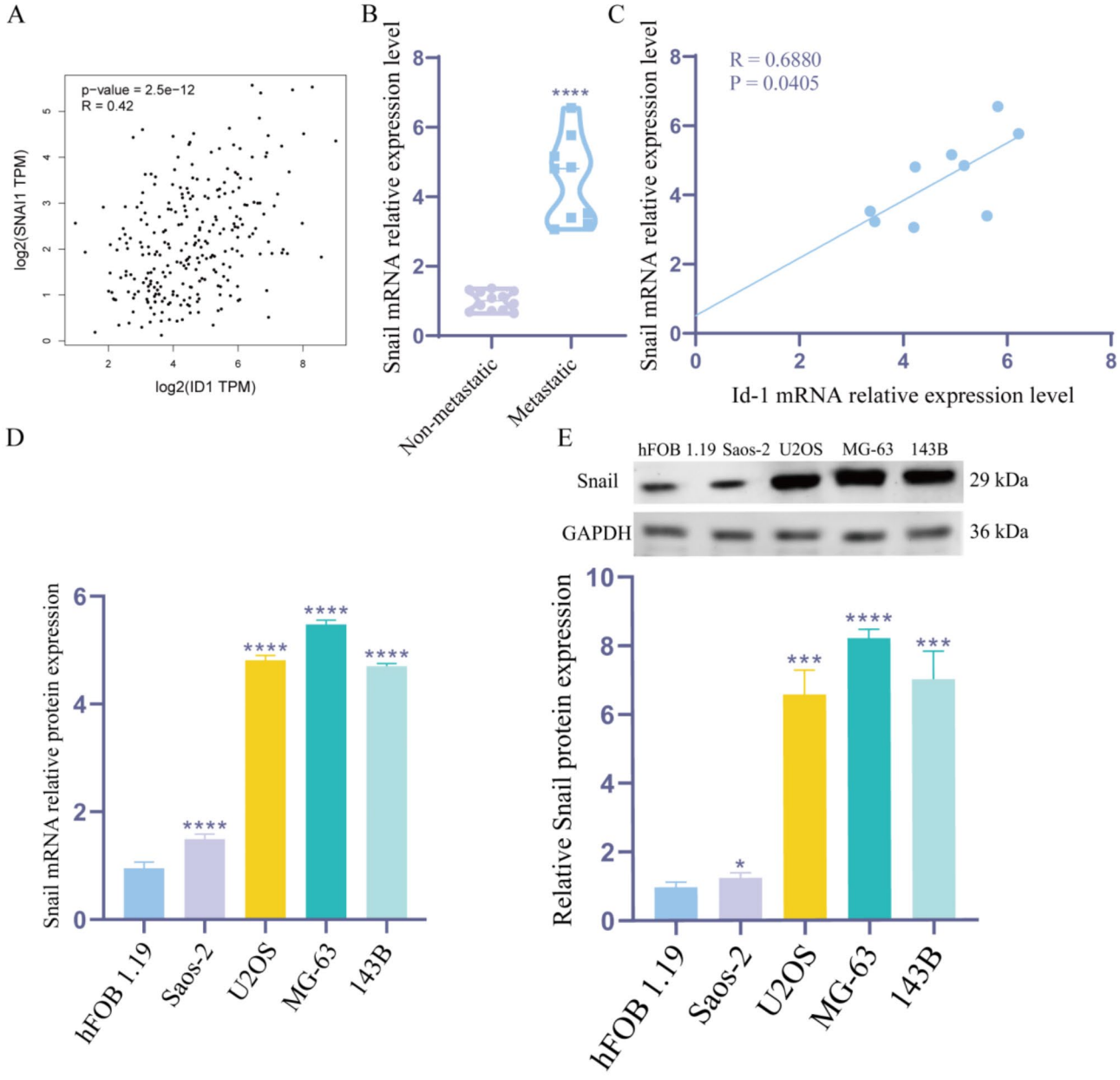

Fig. 2 Snail is highly expressed in OS and is significantly correlated with the expression of Id-1. (**A**) Correlation between Id-1 and Snail in sarcoma analyzed through GEPIA, $p < 0.0001$, $r = 0.42$; (**B**) RT-qPCR for Snail mRNA expression, (Non-metastatic, $n = 12$; Metastatic, $n = 9$), data results were analyzed using t-test, ***$p < 0.001$ vs. non-metastatic; (**C**) Correlation between Id-1 and Snail in metastatic osteosarcoma, $n = 9$, data results were analyzed using pearson correlation analysis, $p = 0.0429$, $r = 0.6824$; (**D**) RT-qPCR for Snail mRNA expression; (**E**) WB for Snail protein content. $n = 3$, data results were analyzed using one-way ANOVA, *$p < 0.05$ vs. hFOB1.19, ***$p < 0.001$ vs. hFOB1.19, ****$p < 0.0001$ vs. hFOB1.19

showed no significant difference ($P > 0.05$), in the sh-Id-1 group, there was no significant difference in body weight, but the tumor volume was significantly smaller. ($P < 0.05$). Observation of the tumor microenvironment revealed that in the Control and sh-NC groups, tumor cells were densely arranged with large and deeply stained nuclei. Tumor cells invaded the normal bone tissue, forming irregular infiltrative borders, and numerous irregular vascular structures were observed within the tumor tissue. Areas of acellular necrosis were visible within the tumor, surrounded by traces of calcification. In comparison to the sh-NC group, the sh-Id-1 group exhibited reduced nuclear pleomorphism, less invasion and disruption of surrounding normal bone tissue, fewer newly formed blood vessels with relatively regular structures, and significantly reduced calcification (Fig. 4D). Further investigation of lung metastasis revealed a significant decrease in the number of visible metastatic nodules on the lung

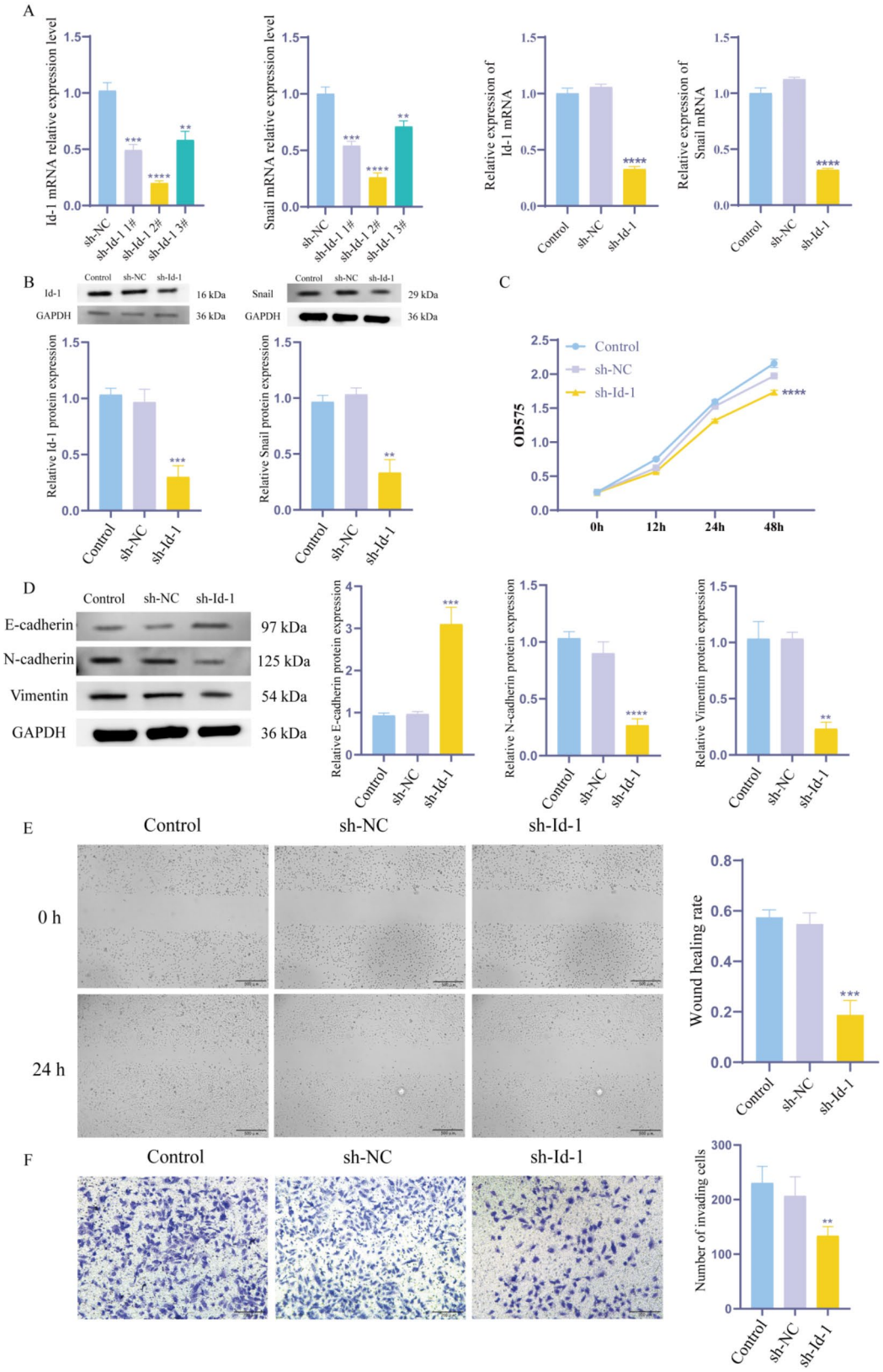

Fig. 3 Silencing Id-1 reduces Snail expression and inhibits EMT in OS cells. (**A**) RT-qPCR for Id-1 and Snail mRNA expression; (**B**) WB for Id-1 and Snail protein content; (**C**) Cell proliferation was assessed using the MTT assay; (**D**) WB for E-cadherin, N-cadherin and Vimentin protein content; (**E**) Cell Scratch Assay for cell migration(100×, scale = 400 μm); (**F**) Transwell for cell invasion(200×, scale = 200 μm). $n = 3$, data results were analyzed using one-way ANOVA, $^{**}p < 0.01$ vs. sh-NC, $^{***}p < 0.001$ vs. sh-NC, $^{****}p < 0.0001$ vs. sh-NC

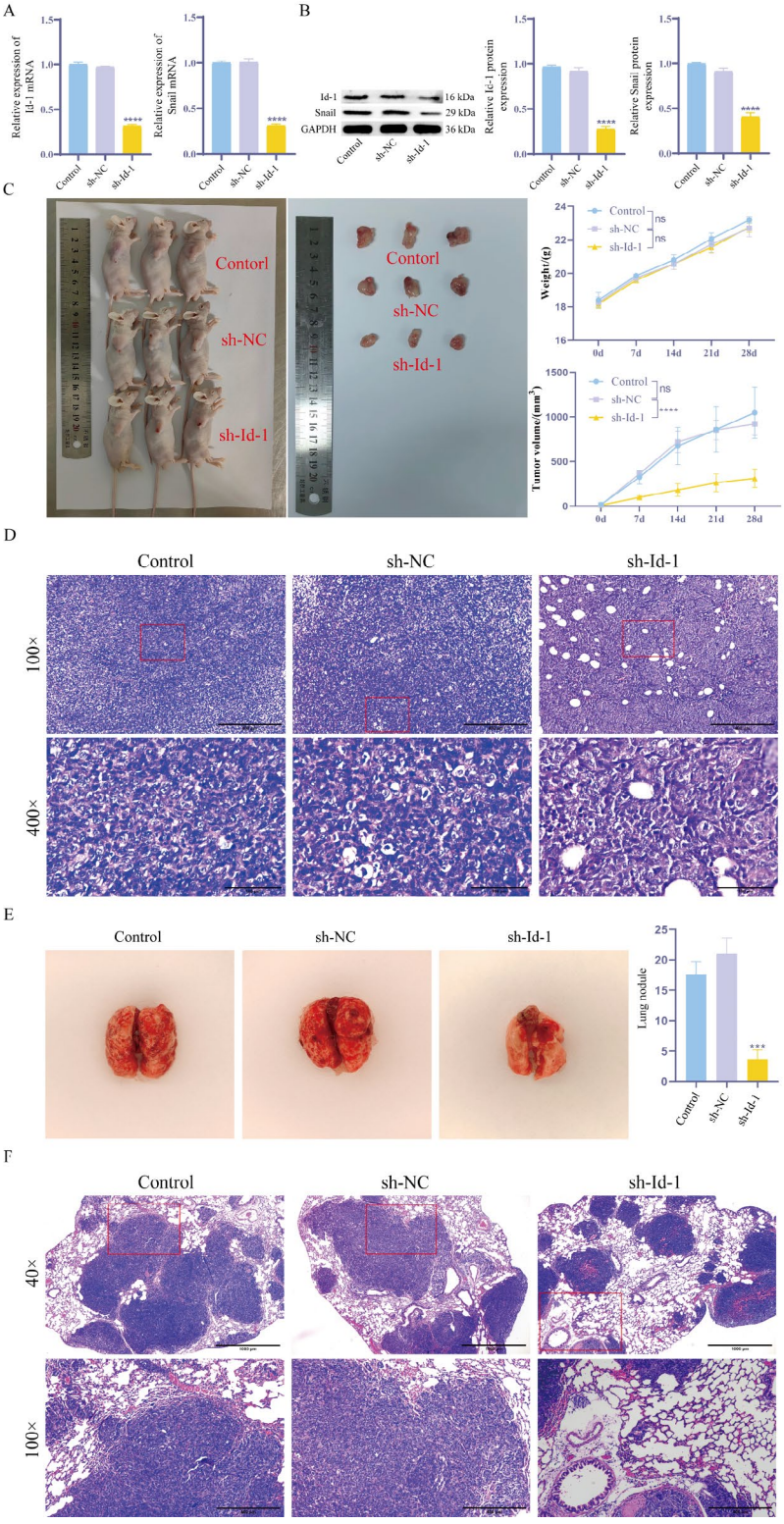

Fig. 4 Downregulation of Id-1 can improve the growth of subcutaneous tumors and lung metastasis in OS mice. (**A**) RT-qPCR for Id-1 and Snail mRNA expression; (**B**) WB for Id-1 and Snail protein content; (**C**) OS cell-injected mice tibia treated to observe the changes of body weight and osteosarcoma volume, data results were analyzed using two-way ANOVA; (**D**) HE to observe OS tumour pathology(100×, scale = 400 μm; 400×, scale = 100 μm); (**E**) number of surface nodules on lung tissue; (**F**) HE to observe lung histopathology(40×, scale = 1000 μm; 100×, scale = 400 μm). $n = 6$, data results were analyzed using one-way ANOVA, *$p < 0.05$ vs. sh-NC, ***$p < 0.001$ vs. sh-NC, ****$p < 0.0001$ vs. sh-NC

surface in the sh-Id-1 group compared to the sh-NC group (Fig. 4E) ($P<0.01$). Lung tissue in the sh-Id-1 group exhibited reduced tumor cell infiltration, relatively preserved alveolar structures, and decreased areas of necrosis and inflammation (Fig. 4F). These results indicate that downregulation of Id-1 effectively inhibits the growth, invasion, and lung metastasis of OS tumors.

Id-1 knockdown inhibits the expression of snail and EMT-associated proteins in OS mice

This study further verified the effect of Id-1 on the expression of Snail and EMT in vivo. Silencing of Id-1 was found to significantly reduce the expression of both Id-1 and Snail in mouse lung tissues by WB and immunohistochemical assays (Fig. 5A, C) ($P<0.01$). Further testing by WB and immunohistochemistry, it was found that compared to the Control group, the sh-NC group showed no significant difference ($P>0.05$). However, in the sh-Id-1 group, E-cadherin was significantly upregulated, while vimentin, N-cadherin, Id-1, and Snail were significantly downregulated (Fig. 5B, D) ($P<0.01$). These results indicate that downregulation of Id-1 effectively reduces the expression of Snail and EMT-related proteins in the lung tissues of OS lung metastasis mouse models.

Discussion

OS is a highly malignant and invasive primary bone tumor that predominantly affects adolescents and young adults, with a significant potential for metastasis, particularly to the lungs [18]. Traditional treatment strategies for this tumor rely heavily on surgical resection and adjuvant chemotherapy, yet its high metastatic rate and recurrence still result in poor prognosis [19]. Therefore, investigating the mechanisms underlying OS metastasis and identifying potential therapeutic targets is crucial.

Id-1, as a transcription factor, has been found to be overexpressed in various tumors and closely associated with tumor invasion and metastasis [20, 21]. Studies by Wong et al. have shown upregulation of Id-1 expression in many cancers [22]. Our research also indicates that Id-1 expression is significantly higher in OS tissues compared to normal bone tissues. Importantly, we found a positive correlation between Id-1 expression and Snail expression in OS tissues. Further investigation revealed that downregulation of Id-1 significantly reduces Snail expression in OS cells. Snail is a key transcription factor that promotes the EMT process [17, 23, 24]. This suggests that Id-1 may influence EMT in OS by regulating Snail expression.

EMT is one of the crucial mechanisms by which tumor cells acquire migratory and invasive capabilities [25]. During EMT, epithelial cells lose their polarity and cell-cell adhesion properties, transitioning to a mesenchymal-like state with increased invasiveness and motility [26]. Key hallmarks of EMT include upregulation of mesenchymal markers (such as vimentin and N-cadherin) and downregulation of epithelial markers (such as E-cadherin) [27]. In this study, silencing of Id-1 led to significant upregulation of E-cadherin and downregulation of vimentin and N-cadherin in OS cells, consistent with the results of cell scratch and Transwell assays. This further illustrates that high Id-1 expression in OS may promote EMT by regulating Snail expression, while Id-1 knockdown can suppress cell migration and invasion in OS. OS is prone to distant metastasis, particularly to the lungs [28]. In vivo studies further demonstrated that silencing Id-1 significantly reduced the number of metastatic nodules on the lung surface, decreased tumor cell infiltration in lung tissue, preserved lung alveolar structure, and reduced areas of necrosis and inflammation. This indicates that Id-1 plays a crucial role in OS lung metastasis regulation, and targeted inhibition of Id-1 may serve as a therapeutic approach against OS metastasis. Pulmonary metastasis of osteosarcoma (OS) is a complex process regulated by multiple pathways. In addition to the Id-1/Snail pathway explored in this study, other pathways are also involved in the regulation of OS pulmonary metastasis. For instance, research by Wang et al. has shown that targeting the CK1α/CBX4 axis may be effective in treating OS lung metastasis [29]. Zhu et al. discovered that the Wnt/β-catenin signaling pathway is related to OS pulmonary metastasis [30]. Future studies could further explore other potential pathways involved in OS metastasis to comprehensively elucidate the mechanisms of OS metastasis.

In conclusion, this study systematically elucidated for the first time the critical role of Id-1 and Snail in OS invasion and metastasis, providing new therapeutic targets for the treatment of OS. These findings lay the groundwork for the development of precise therapeutic strategies against OS and also serve as a reference for research on other types of cancers.

Conclusion

Downregulation of Id-1 inhibits the EMT process by reducing Snail expression, thereby effectively suppressing the growth, invasion, and lung metastasis of OS. This study systematically elucidates the critical role of Id-1 in OS invasion and metastasis, providing Id-1 as a new therapeutic targets.

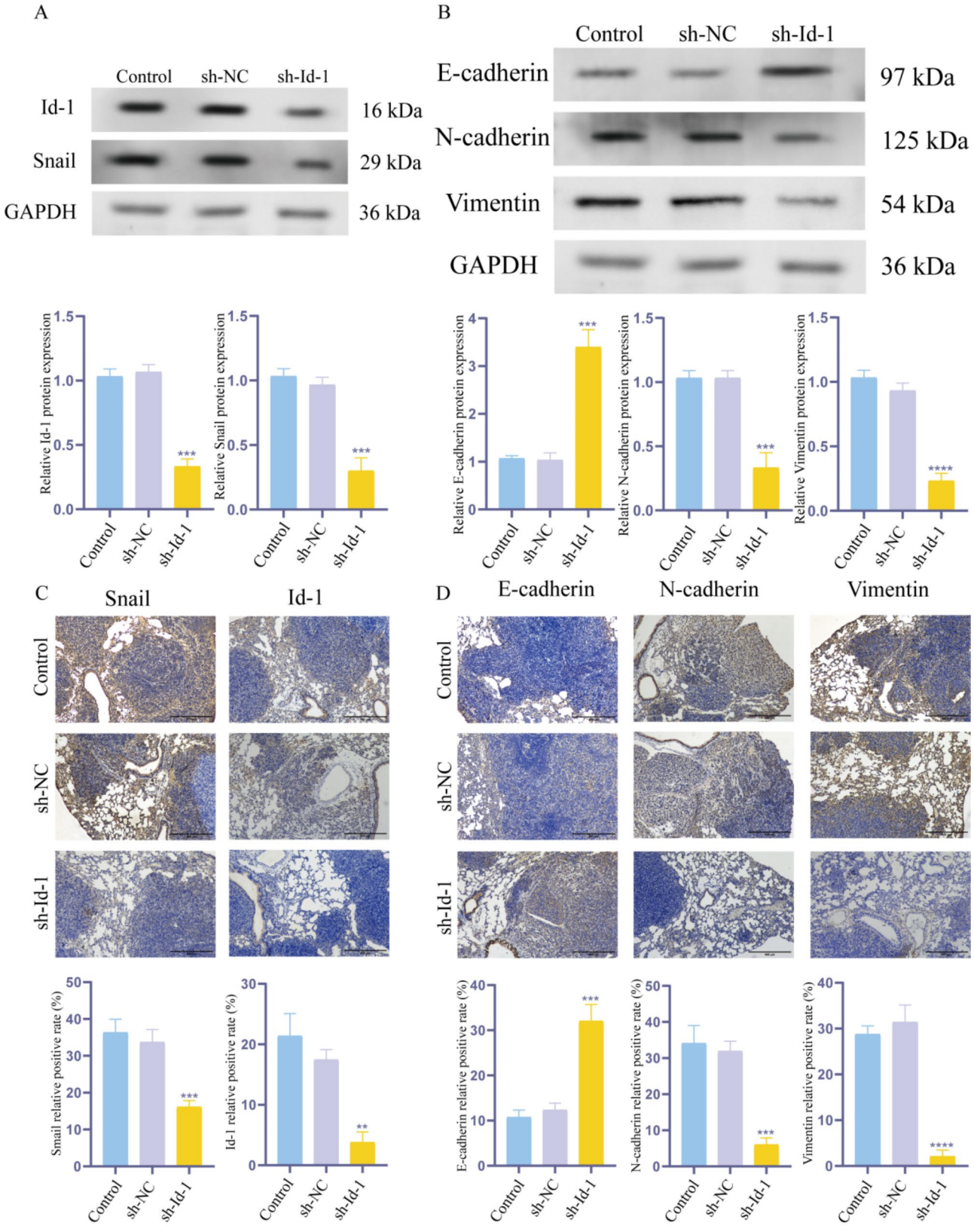

Fig. 5 Id-1 knockdown inhibits the expression of Snail and EMT-associated proteins in OS mice (**A**) WB detected the protein expression of Id-1 and Snail; (**B**) WB detected the protein expression of E-cadherin, N-cadherin and Vimentin; (**C**) IHC detected the protein expression of Id-1 and Snail (100×, scale = 400 μm); (**D**) IHC detected the protein expression of E-cadherin, N-cadherin and Vimentin (100×, scale = 400 μm). $n = 6$, data results were analyzed using one-way ANOVA, $^{**}p < 0.01$ vs. sh-NC, $^{***}p < 0.001$ vs. sh-NC, $^{****}p < 0.0001$ vs. sh-NC

Author contributions
Rongbing Shu and Zhuanyi Yu have contributed equally to this work and share first authorship. They were involved in the conception, design, and execution of the study, as well as the analysis and interpretation of the data. Jianmin Wu and Qiuxin Cheng contributed to the acquisition of data and provided essential technical support. Zhihao Peng and Huaqiang Zhou assisted in the interpretation of data and critically revised the manuscript for important intellectual content. Min Zhao, as the corresponding author, provided the overall guidance and supervision of the project, and was responsible for the final approval of the version to be published. All authors have read and approved the final manuscript.

Funding
It is supported by Yingtan Science and Technology Plan Project: Provincial Special Fund for Guiding Local Science and Technology Development in 2024 (Free Exploration Basic Research)(No.202412 – 18894), Science and Technology Program of Health Commission of Jiangxi Province (No.SKJP1220243837) and Yingtan People's Hospital Hospital Level Plan Project.

Data availability
No datasets were generated or analysed during the current study.

Declarations

Ethics approval and consent to participate
This study strictly adhered to the 3R principle and was approved by the Animal Committee of Yingtan People's Hospital(Ethics No.YT202413). All patients signed informed consent forms, and the study was conducted under the supervision of the Ethics Committee of Yingtan People's Hospital (YT2024101).

Competing interests
The authors declare no competing interests.

Author details
[1]Department of Orthopedic, Yingtan People's Hospital, Yingtan 335000, Jiangxi, China

Received: 28 October 2024 / Accepted: 24 December 2024
Published online: 31 January 2025

References

1. Meltzer PS, Helman LJ. New Horizons in the Treatment of Osteosarcoma. N Engl J Med. 2021;385(22):2066–76.
2. Kansara M, et al. Translational biology of osteosarcoma. Nat Rev Cancer. 2014;14(11):722–35.
3. Jiang Y, et al. KDM6B-mediated histone demethylation of LDHA promotes lung metastasis of osteosarcoma. Theranostics. 2021;11(8):3868–81.
4. Chen C, et al. Immunotherapy for osteosarcoma: fundamental mechanism, rationale, and recent breakthroughs. Cancer Lett. 2021;500:1–10.
5. Zhang Y, et al. Down-regulation of Skp2 expression inhibits invasion and lung metastasis in osteosarcoma. Sci Rep. 2018;8(1):14294.
6. Gundamaraju R, et al. Autophagy and EMT in cancer and metastasis: who controls whom? Biochim Biophys Acta Mol Basis Dis. 2022;1868(9):166431.
7. Park M et al. Breast Cancer metastasis: mechanisms and therapeutic implications. Int J Mol Sci, 2022; 23(12).
8. Diepenbruck M, Christofori G. Epithelial-mesenchymal transition (EMT) and metastasis: yes, no, maybe? Curr Opin Cell Biol. 2016;43:7–13.
9. Wu XL, et al. Id-1 expression in colorectal adenocarcinoma tissues and its clinical significance. Rev Assoc Med Bras. 2019;65(3):404–9.
10. Hao L, et al. Id-1 promotes osteosarcoma cell growth and inhibits cell apoptosis via PI3K/AKT signaling pathway. Biochem Biophys Res Commun. 2016;470(3):643–9.
11. Hui CM, et al. Id-1 promotes proliferation of p53-deficient esophageal cancer cells. Int J Cancer. 2006;119(3):508–14.
12. Schindl M, et al. Level of Id-1 protein expression correlates with poor differentiation, enhanced malignant potential, and more aggressive clinical behavior of epithelial ovarian tumors. Clin Cancer Res. 2003;9(2):779–85.
13. Luo D, et al. Tongue squamous cell carcinoma resists hyperthermia treatment by promoting Id-1 expression mediated EMT. Bull Cancer. 2022;109(9):886–94.
14. Guo S, et al. Acupuncture and Moxibustion Inhibited Intestinal Epithelial-Mesenchymal Transition in patients with Crohn's Disease Induced by TGF- β 1/Smad3/Snail pathway: a clinical Trial Study. Chin J Integr Med. 2022;28(9):823–32.
15. Chen C, et al. VIRMA facilitates triple-negative breast Cancer Progression via increasing m6A-Dependent KIF15 expression. Discov Med. 2023;35(178):787–95.
16. Eaton BR, et al. Osteosarcoma Pediatr Blood Cancer. 2021;68(Suppl 2):e28352.
17. Shoaib Z, Fan TM, Irudayaraj JMK. Osteosarcoma mechanobiology and therapeutic targets. Br J Pharmacol. 2022;179(2):201–17.
18. El-Sokkary GH, Ismail IA, Saber SH. Melatonin inhibits breast cancer cell invasion through modulating DJ-1/KLF17/ID-1 signaling pathway. J Cell Biochem. 2019;120(3):3945–57.
19. Han L, et al. MicroRNA-338-5p reverses chemoresistance and inhibits invasion of esophageal squamous cell carcinoma cells by targeting Id-1. Cancer Sci. 2019;110(12):3677–88.
20. Chang J, et al. Intratibial osteosarcoma cell injection to generate orthotopic osteosarcoma and lung metastasis mouse models. J Vis Exp. 2021;(176).
21. Bao Z, et al. SNAIL induces EMT and lung metastasis of Tumours secreting CXCL2 to promote the Invasion of M2-Type immunosuppressed macrophages in Colorectal Cancer. Int J Biol Sci. 2022;18(7):2867–81.
22. Bao Z, et al. SNAIL induces EMT and lung metastasis of Tumours secreting CXCL2 to promote the Invasion of M2-Type immunosuppressed macrophages in Colorectal Cancer. Int J Biol Sci. 2022;18(7):2867–81.
23. Han JH, et al. Snail acetylation by autophagy-derived acetyl-coenzyme A promotes invasion and metastasis of KRAS-LKB1 co-mutated lung cancer cells. Cancer Commun (Lond). 2022;42(8):716–49
24. Wong YC, Wang X, Ling MT. Id-1 expression and cell survival. Apoptosis. 2004;9(3):279–89.
25. Sadrkhanloo M, et al. STAT3-EMT axis in tumors: modulation of cancer metastasis, stemness and therapy response. Pharmacol Res. 2022;182:106311.
26. Pastushenko I, Blanpain C. EMT transition states during tumor progression and metastasis. Trends Cell Biol. 2019;29(3):212–26.
27. Huang Y, Hong W, Wei X. The molecular mechanisms and therapeutic strategies of EMT in tumor progression and metastasis. J Hematol Oncol. 2022;15(1):129.
28. Yu S, et al. Lung cells support osteosarcoma cell migration and survival. BMC Cancer. 2017;17(1):78.
29. Wang X, et al. Targeting the CK1α/CBX4 axis for metastasis in osteosarcoma. Nat Commun. 2020;11(1):1141.
30. Zhu H, et al. Melittin inhibits lung metastasis of human osteosarcoma: evidence of wnt/β-catenin signaling pathway participation. Toxicon. 2021;198:132–42.

Publisher's note